Ferromagnetism in the multiband Kondo lattice model

A. Sharma* and W. Nolting
Institut für Physik, Humboldt-Universität zu Berlin, Newtonstr. 15, 12489, Berlin, Germany
(Received 28 January 2008; revised manuscript received 13 June 2008; published 1 August 2008)

The ferromagnetic spin-exchange interaction between the itinerant electrons and localized moments on a periodic lattice, studied within the so-called Kondo lattice model, is considered for multiband situation where the hopping integral is a matrix in general. The modified Ruderman-Kittel-Kasuya-Yosida theory, wherein one can map such a model onto an effective Heisenberg-type system, is extended to a multiband case with finite bandwidth and hybridization on a simple-cubic lattice. As an input for the evaluation of the effective exchange integrals, one requires the multiband electronic self-energy, which is taken from an earlier proposed ansatz. Using the above procedure, we determine the magnetic properties of the system such as Curie temperature while calculating the chemical potential and magnetization within a self-consistent scheme for various values of system parameters. The results are discussed in detail and the model is motivated in order to study the electronic, transport, and magnetic properties of real materials like GdN.

DOI: 10.1103/PhysRevB.78.054402 PACS number(s): 71.10.−w, 71.27.+a, 75.10.−b

I. INTRODUCTION

The original *Kondo model* with antiferromagnetic spin-exchange interaction between a single impurity spin in a nonmagnetic background and the itinerant electrons of the host metal was used by Kondo[1] to explain the unusual temperature behavior of the resistivity of the system. Its periodic extension with ferromagnetic exchange interaction between a system of localized spins and a band of itinerant electrons is in the literature often referred to as the *ferromagnetic Kondo lattice model*[2,3] or *s-d* (Refs. 4 and 5) or *s-f* model.[6] For the sake of uniformity, we ascribe it as the *Kondo lattice model* (KLM). Both the antiferromagnetic as well as the ferromagnetic alignment of itinerant and localized spins exhibits remarkable differences in the physical properties of various real materials and has been a subject of intense theoretical studies in the past.

For instance, the magnetic semiconductors (prototypes being the europium chalcogenides: EuX: X=O,S,Se,Te) (Refs. 7–9) are known to have ferromagnetic exchange coupling and demonstrate a spectacular temperature dependence of the band states. The redshift of the optical-absorption edge in these materials upon cooling from $T=T_c$ to $T=0$ K is due to a corresponding shift of the lower conduction-band edge.[8,10] A great deal of focus has been concentrated on studying the diluted magnetic semiconductors with antiferromagnetic[11] and ferromagnetic[12,13] exchange interactions with the purpose of achieving practical spintronics[14,15] applications. Apart from magnetic semiconductors, the local-moment metals like Gd are known to have a ferromagnetic exchange.[16] But the exchange-induced correlation and the temperature-dependent quasiparticle effects[17] have lead to complex and hence controversial photoemission data.[18,19] Other materials such as the manganese oxides (manganites) having pervoskite structures (the prototype being $A_{1-x}B_xMnO_3$ where A=La,Pr,Nd and B=Sr,Ca,Ba,Pb) also have a strong ferromagnetic exchange interaction. They have a remarkable property called colossal magnetoresistance (CMR),[20,21] which enables them to dramatically change their electrical resistance in the presence of a magnetic field. Many theoretical models have been proposed in order to explain the existence of these effects. The earlier theoretical ideas were based on the double exchange model,[22] which can be understood as one of the limiting cases of Kondo lattice model (i.e., limit of strong Hunds coupling). Although recent theories[23] have provided a step forward, its complete understanding is far from being explained by any current physical theories. As compared to the aforementioned compounds, the heavy fermion systems[24] (mostly Ce compounds) are known to have antiparallel alignment of the conduction electron and localized spins. They have been rigorously studied because of their extraordinary physical properties.[25]

In the above examples, the kinetic energy of the itinerant electrons is usually described within tight-binding dispersion of a single nondegenerate band, i.e., single orbital atom per unit cell. But it is well known that the single-band calculations are certainly not sufficient in order to have a complete understanding of unusual phenomenon in real materials.[26] One has to take into account the intraband and interband interactions as well.

The multiband models are also of growing interest for exhibiting a wide range of phenomena such as novel electronic phases, magnetism, and superconductivity.[27] For instance, it was found out using a two-band Hubbard[28] model that there was a possibility of existence of ferromagnetism around half-filling[29] in contrast to antiferromagnetism in the single-band model.[30] The numerical studies[31] on ground-state properties of multiband periodic Anderson[32] model revealed the minor role played by the competition between Ruderman-Kittel-Kasuya-Yosida (RKKY) (Ref. 33) and Kondo interactions[1] again in contrast to the single-band case.[34] This motivates us to understand the physics behind the interplay between the kinetic and potential energy of multiband Kondo lattice model and extend it for studying the electronic, transport, and magnetic properties of real materials such as GdN.

This paper is organized as follows. In Sec. II we develop our theoretical multiband model Hamiltonian describing the physics due to the intra-atomic exchange interaction between the two subsystems, i.e., itinerant electrons and localized spins on a periodic lattice. In Sec. II A, we consider only the

electronic part of the system while treating the magnetic part within molecular-field theory. Using an earlier proposed ansatz for multiband self-energy,[35] we evaluate the electronic properties of interest such as the density of states and band occupation number. In Sec. II B, we develop the modified RKKY theory[36] wherein we integrate out the charge degrees of freedom of the itinerant electrons thereby mapping the multiband Kondo lattice Hamiltonian onto an effective Heisenberg-type spin Hamiltonian. In Sec. III, using the procedure described in Sec. II, we determine the magnetic properties of the system such as Curie temperature while calculating the chemical potential and magnetization within a self-consistent scheme. We discuss the results obtained for various values of system parameters. In Sec. IV, we summarize and conclude our findings.

II. MODEL AND METHODS

A. Electronic subsystem

In this section, we present a brief description of the theoretical model used in our calculations. The details of the many-body analysis along with a model calculation and limiting cases are explained elsewhere.[35] The multiband KLM Hamiltonian mainly consists of two parts;

$$H = H_{\mathrm{kin}} + H_{\mathrm{int}}, \tag{1}$$

where

$$H_{\mathrm{kin}} = \sum_{ij\alpha\beta\sigma} T_{ij}^{\alpha\beta} c_{i\alpha\sigma}^{\dagger} c_{j\beta\sigma}, \tag{2}$$

and

$$H_{\mathrm{int}} = -\frac{J}{2} \sum_{\substack{i\alpha \\ \sigma'\sigma}} (\mathbf{S}_i \cdot \boldsymbol{\sigma})_{\sigma'\sigma} c_{i\alpha\sigma'}^{\dagger} c_{i\alpha\sigma}. \tag{3}$$

H_{kin} denotes the kinetic energy of the itinerant electrons with $T_{ij}^{\alpha\beta}$ being the hopping term, which is connected by Fourier transformation to the free Bloch energies $\epsilon^{\alpha\beta}(\mathbf{k})$;

$$T_{ij}^{\alpha\beta} = \frac{1}{N} \sum_{\mathbf{k}} \epsilon^{\alpha\beta}(\mathbf{k}) e^{-i\mathbf{k}\cdot(R_i - R_j)}, \tag{4}$$

while $c_{i\alpha\sigma}^{\dagger}$ and $c_{i\alpha\sigma}$ are the fermionic creation and annihilation operators, respectively, at lattice site R_i. The latin letters $(i,j, \ldots)$ symbolize the crystal lattice indices while the band indices are depicted in Greek letters $(\alpha,\beta, \ldots)$ and the spin is denoted as $\sigma(=\uparrow,\downarrow)$.

H_{int} is an intra-atomic exchange interaction term, i.e., a local interaction between electron spin $\boldsymbol{\sigma}$ and local-moment spin S_i. Using second quantization for electron spin $(n_{i\alpha\sigma} = c_{i\alpha\sigma}^{\dagger} c_{i\alpha\sigma})$, the interaction term is further being split into two subterms.

$$H_{\mathrm{int}} = -\frac{J}{2} \sum_{i\alpha\sigma} (z_\sigma S_i^z c_{i\alpha\sigma}^{\dagger} c_{i\alpha\sigma} + S_i^{\sigma} c_{i\alpha-\sigma}^{\dagger} c_{i\alpha\sigma}). \tag{5}$$

The first term describes the Ising-type interaction between the z component of the localized and itinerant carrier spins while the other term comprises spin-exchange processes, which are responsible for many of the KLM properties. J is the exchange coupling strength, which we assume to be $\mathbf{k}$ independent and S_i^{σ} refers to the localized spin at site R_i;

$$S_i^{\sigma} = S_i^x + i z_\sigma S_i^y; \quad z_\uparrow = +1, \quad z_\downarrow = -1. \tag{6}$$

The Hamiltonian in Eq. (1) provokes a nontrivial many-body problem that cannot be solved exactly. Using the equation of motion method for the double-time retarded Green's function[37]

$$G_{lm\sigma}^{\mu\nu}(E) = \langle\langle c_{l\mu\sigma}; c_{m\nu\sigma}^{\dagger} \rangle\rangle_E, \tag{7}$$

where l,m and μ,ν are the lattice and band indices, respectively, we obtain higher-order Green's functions, which prevent the direct solution. Approximations must be considered. But a rather formal solution can be stated as

$$\hat{G}_{\mathbf{k}\sigma}(E) = [(E + i0^+)\hat{I} - \hat{\epsilon}(\mathbf{k}) - \hat{\Sigma}_{\mathbf{k}\sigma}(E)]^{-1}, \tag{8}$$

where, for simplicity, we exclude the band indices by representing the terms in a generalized matrix form on symbolizing a hat over it;

$$\hat{G}_{lm\sigma}(E) = \frac{1}{N} \sum_{\mathbf{k}} \hat{G}_{\mathbf{k}\sigma}(E) e^{-i\mathbf{k}\cdot(R_l - R_m)}. \tag{9}$$

The terms in Eq. (8) are explained as follows: $\hat{I}$ is an identity matrix. 0^+ is a small imaginary part and $\hat{\epsilon}(\mathbf{k})$ is a hopping matrix with the diagonal terms of the matrix exemplifying the intraband hopping and the off-diagonal terms denoting the interband hopping. The self-energy $\hat{\Sigma}_{\mathbf{k}\sigma}$(E) containing all the influences of the different interactions being of fundamental importance can be understood using site representation

$$\langle\langle [H_{\mathrm{int}}, c_{l\mu\sigma}]_-; c_{m\nu\sigma}^{\dagger} \rangle\rangle = \sum_{p\gamma} \Sigma_{lp\sigma}^{\mu\gamma}(E) G_{pm\sigma}^{\gamma\nu}(E). \tag{10}$$

Now we are left with a problem of finding a multiband self-energy ansatz in order to compute the Green's function matrix and thereby to calculate the physical quantities of interest such as the quasiparticle spectral density (SD)

$$S_{\mathbf{k}\sigma}(E) = -\frac{1}{\pi} \mathrm{Im\ Tr}(\hat{G}_{\mathbf{k}\sigma}(E)) \tag{11}$$

and the quasiparticle density of states (QDOS)

$$\rho_\sigma(E) = \frac{1}{N\hbar} \sum_{\mathbf{k}} S_{\mathbf{k}\sigma}(E), \tag{12}$$

which would yield the band occupation number

$$n = \sum_\sigma n_\sigma = \int_{-\infty}^{\infty} dE f_-(E) \rho_\sigma(E), \tag{13}$$

where

$$f_{-}(E) = \frac{1}{e^{\frac{E-\mu}{k_B T}} + 1}$$

is the Fermi function and μ is the chemical potential or the Fermi edge.

According to our many-body theoretical analysis,[35] we utilize the multiband interpolating self-energy ansatz (ISA), which is well defined in the low carrier density regime[38] for all coupling strengths and satisfy one limiting case of the model, namely, that of ferromagnetically saturated semiconductor. The ansatz is given as

$$\hat{\Sigma}_\sigma(E) = \frac{J}{2} M_{-\sigma} \hat{I} + \frac{J^2}{4} a_{-\sigma} \hat{G}_{-\sigma}\left(E + \frac{J}{2} M_{-\sigma}\right) \times \left[\hat{I} - \frac{J}{2} \hat{G}_{-\sigma}\left(E + \frac{J}{2} M_{-\sigma}\right)\right]^{-1}, \tag{14a}$$

where

$$M_\sigma = z_\sigma \langle S^z \rangle; \quad a_\sigma = S(S+1) + M_\sigma (M_\sigma + 1) \tag{14b}$$

and the bare Green's function matrix is defined as

$$\hat{G}_\sigma(E) = \frac{1}{N} \sum_{\mathbf{k}} [(E + i0^+)\hat{I} - \hat{\epsilon}(\mathbf{k})]^{-1}.$$

The first term in Eq. (14a), which is exact in the weak-coupling limit, represents an induced *Stoner splitting* of the energy band proportional to the f spin magnetization $\langle S^z \rangle$. The second term is dominated by the consequences of spin-exchange processes between itinerant electrons and localized f moments.

As seen in Eq. (14a), we are interested only in the local self-energy

$$\hat{\Sigma}_\sigma(E) = \frac{1}{N} \sum_{\mathbf{k}} \hat{\Sigma}_{\mathbf{k}\sigma}(E),$$

while the wave-vector dependence of the self-energy is mainly due to the magnon energies appearing at finite temperature. In order to evaluate only the itinerant electron subsystem, we can neglect this wave-vector dependence. The localized magnetization $\langle S^z \rangle$ can then be considered as an external parameter being responsible for the induced temperature dependence of the band states. Thus, in a non-self-consistent way, it is possible to determine the influence of interband exchange on the conduction-band states so as to study the electronic correlations effects.[35,38] But in order to study the effect of itinerant electron subsystem on the localized subsystem and vice versa, we need to calculate the magnetization within a self-consistent manner as shown in Sec. II B.

B. Magnetic subsystem

In Sec. II A, we did not consider a direct exchange interaction between the localized f spins. But if one is interested in determining the magnetic properties of multiband KLM, then both the subsystems (localized as well as itinerant) should be solved within a self-consistent scheme.

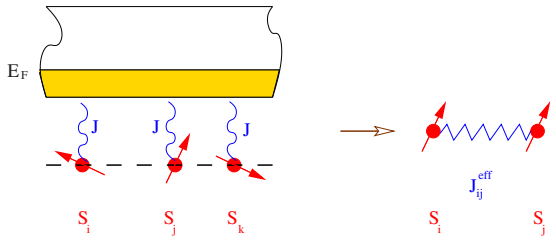

FIG. 1. (Color online) An effective indirect exchange J_{ij}^{eff} between localized f spins (red arrows) mediated by intra-atomic exchange J due to itinerant electrons. E_F denotes the Fermi edge.

Therefore, we would like to take into account an effective indirect coupling J_{ij}^{eff} between the localized f spins and the itinerant electrons within the so-called modified RKKY (Ref, 36) formalism as shown in Fig. 1.

Consider the multiband Kondo lattice Hamiltonian, i.e., Eq. (1), which can be written in the following equivalent form:

$$H = H_{\text{kin}} + H_{\text{int}} = \sum_{\mathbf{k}\alpha\beta\sigma} \epsilon^{\alpha\beta}(\mathbf{k}) c^\dagger_{\mathbf{k}\alpha\sigma} c_{\mathbf{k}\beta\sigma} - \frac{J}{2N} \sum_{i\alpha} \sum_{\mathbf{kq}} \sum_{\sigma'\sigma} e^{-i\mathbf{q}\cdot\mathbf{R}_i} (\mathbf{S}_i \cdot \boldsymbol{\sigma})_{\sigma'\sigma} c^\dagger_{\mathbf{k}+\mathbf{q}\alpha\sigma'} c_{\mathbf{k}\alpha\sigma},$$

where all the terminologies remain the same as explained in Sec. II A. The components of the band electron-spin operator $\boldsymbol{\sigma}$ are the Pauli-spin matrices.

The main idea of the modified RKKY theory is to transform the above Kondo-type exchange Hamiltonian of the conduction electrons into an effective Heisenberg-type spin-exchange Hamiltonian of the f spins by averaging H_{int} in the subspace of the conduction electrons ($\langle\ \rangle$);

$$\langle H_{\text{int}} \rangle = H_f = -\frac{J}{2N} \sum_{i\alpha} \sum_{\mathbf{kq}} \sum_{\sigma'\sigma} e^{-i\mathbf{q}\cdot\mathbf{R}_i} (\mathbf{S}_i \cdot \boldsymbol{\sigma})_{\sigma'\sigma} \langle c^\dagger_{\mathbf{k}+\mathbf{q}\alpha\sigma'} c_{\mathbf{k}\alpha\sigma} \rangle. \tag{15}$$

This is achieved by closely following the treatment given in Ref. 36. For averaging procedure the f spin operators are to be considered as c numbers. The expectation values $\langle\ \rangle$ in Eq. (15) may still have operator properties in the f spin subspace and therefore do not vanish for $\mathbf{q} \neq 0$ and $\sigma \neq \sigma'$. We would like to obtain $\langle\ \rangle$ via the spectral theorem with the help of appropriate Green's function as given below:

$$G^{\alpha\beta\sigma\sigma'}_{\mathbf{k},\mathbf{k}+\mathbf{q}}(E) = \langle\langle c_{\mathbf{k}\alpha\sigma}; c^\dagger_{\mathbf{k}+\mathbf{q}\beta\sigma'} \rangle\rangle_E. \tag{16}$$

Its equation of motion can be obtained in the usual way[37] and is given as

$$E G^{\alpha\beta\sigma\sigma'}_{\mathbf{k},\mathbf{k}+\mathbf{q}}(E) = \delta_{\mathbf{k},\mathbf{k}+\mathbf{q}} \delta_{\alpha\beta} \delta_{\sigma\sigma'} + \sum_\gamma \epsilon^{\alpha\gamma}(\mathbf{k}) G^{\gamma\beta\sigma\sigma'}_{\mathbf{k},\mathbf{k}+\mathbf{q}}(E) - \frac{J}{2N} \sum_{i\mathbf{k}'\sigma''} e^{-i(\mathbf{k}-\mathbf{k}')\cdot\mathbf{R}_i} (\mathbf{S}_i \cdot \boldsymbol{\sigma})_{\sigma\sigma''} G^{\alpha\beta\sigma''\sigma'}_{\mathbf{k}',\mathbf{k}+\mathbf{q}}(E). \tag{17}$$

The above equation can be iterated up to any desired accuracy producing spin products of the type

$$(\mathbf{S}_i \cdot \boldsymbol{\sigma})_{\sigma\sigma''}, \quad (\mathbf{S}_i \cdot \boldsymbol{\sigma})_{\sigma''\sigma'''}, \quad (\mathbf{S}_i \cdot \boldsymbol{\sigma})_{\sigma'''\sigma''''}.$$

On excluding the band indices in Eq. (17) by representing the terms in a generalized matrix form on symbolizing a hat over it we get

$$E\hat{G}^{\sigma\sigma'}_{\mathbf{k},\mathbf{k}+\mathbf{q}}(E) = \delta_{\mathbf{k},\mathbf{k}+\mathbf{q}}\delta_{\sigma\sigma'}\hat{I} + \hat{\epsilon}(\mathbf{k})\hat{G}^{\sigma\sigma'}_{\mathbf{k},\mathbf{k}+\mathbf{q}}(E) - \frac{J}{2N}\sum_{i\mathbf{k}'\sigma''} e^{-i(\mathbf{k}-\mathbf{k}')\cdot\mathbf{R}_i}(\mathbf{S}_i \cdot \boldsymbol{\sigma})_{\sigma\sigma''}\hat{G}^{\sigma''\sigma'}_{\mathbf{k}',\mathbf{k}+\mathbf{q}}(E). \tag{18}$$

Rearranging the terms in Eq. (18) yields

$$[E\hat{I} - \hat{\epsilon}(\mathbf{k})]\hat{G}^{\sigma\sigma'}_{\mathbf{k},\mathbf{k}+\mathbf{q}}(E) = \delta_{\mathbf{k},\mathbf{k}+\mathbf{q}}\delta_{\sigma\sigma'}\hat{I} - \frac{J}{2N}\sum_{i\mathbf{k}'\sigma''} e^{-i(\mathbf{k}-\mathbf{k}')\cdot\mathbf{R}_i} \times (\mathbf{S}_i \cdot \boldsymbol{\sigma})_{\sigma\sigma''}\hat{G}^{\sigma''\sigma'}_{\mathbf{k}',\mathbf{k}+\mathbf{q}}(E). \tag{19}$$

For symmetry reasons, we write down the equation of motion for $G^{\alpha\beta\sigma\sigma'}_{\mathbf{k},\mathbf{k}+\mathbf{q}}(E)$ in an alternative way, where the second operator $c^{\dagger}_{\mathbf{k}+\mathbf{q}\beta\sigma'}$ in Eq. (16) is the "active" operator

$$E\hat{G}^{\sigma\sigma'}_{\mathbf{k},\mathbf{k}+\mathbf{q}}(E) = \delta_{\mathbf{k},\mathbf{k}+\mathbf{q}}\delta_{\sigma\sigma'}\hat{I} + \hat{G}^{\sigma\sigma'}_{\mathbf{k},\mathbf{k}+\mathbf{q}}(E)\hat{\epsilon}(\mathbf{k}+\mathbf{q}) - \frac{J}{2N}\sum_{i\mathbf{k}'\sigma''} e^{-i(\mathbf{k}'-(\mathbf{k}+\mathbf{q}))\cdot\mathbf{R}_i}(\mathbf{S}_i \cdot \boldsymbol{\sigma})_{\sigma''\sigma'}\hat{G}^{\sigma\sigma''}_{\mathbf{k},\mathbf{k}'}(E) \tag{20}$$

and again upon rearranging the terms in the above equation we get

$$\hat{G}^{\sigma\sigma'}_{\mathbf{k},\mathbf{k}+\mathbf{q}}(E)[E\hat{I} - \hat{\epsilon}(\mathbf{k}+\mathbf{q})] = \delta_{\mathbf{k},\mathbf{k}+\mathbf{q}}\delta_{\sigma\sigma'}\hat{I} - \frac{J}{2N}\sum_{i\mathbf{k}'\sigma''} e^{-i[\mathbf{k}'-(\mathbf{k}+\mathbf{q})]\cdot\mathbf{R}_i} \times (\mathbf{S}_i \cdot \boldsymbol{\sigma})_{\sigma''\sigma'}\hat{G}^{\sigma\sigma''}_{\mathbf{k},\mathbf{k}'}(E). \tag{21}$$

Now let us define the following Green's function of the "free" electron system

$$[E\hat{I} - \hat{\epsilon}(\mathbf{k})] = (\hat{G}^{(0)}_{\mathbf{k}}(E))^{-1}, \tag{22}$$

$$[E\hat{I} - \hat{\epsilon}(\mathbf{k}+\mathbf{q})] = (\hat{G}^{(0)}_{\mathbf{k}+\mathbf{q}}(E))^{-1}. \tag{23}$$

Substituting Eq. (22) in Eq. (19) gives

$$(\hat{G}^{(0)}_{\mathbf{k}}(E))^{-1}\hat{G}^{\sigma\sigma'}_{\mathbf{k},\mathbf{k}+\mathbf{q}}(E) = \delta_{\mathbf{k},\mathbf{k}+\mathbf{q}}\delta_{\sigma\sigma'}\hat{I} - \frac{J}{2N}\sum_{i\mathbf{k}'\sigma''} e^{-i(\mathbf{k}-\mathbf{k}')\cdot\mathbf{R}_i} \times (\mathbf{S}_i \cdot \boldsymbol{\sigma})_{\sigma\sigma''}\hat{G}^{\sigma''\sigma'}_{\mathbf{k}',\mathbf{k}+\mathbf{q}}(E), \tag{24}$$

while substituting Eq. (23) in Eq. (21) yields

$$\hat{G}^{\sigma\sigma'}_{\mathbf{k},\mathbf{k}+\mathbf{q}}(E)(\hat{G}^{(0)}_{\mathbf{k}+\mathbf{q}}(E))^{-1} = \delta_{\mathbf{k},\mathbf{k}+\mathbf{q}}\delta_{\sigma\sigma'}\hat{I} - \frac{J}{2N}\sum_{i\mathbf{k}'\sigma''} e^{-i[\mathbf{k}'-(\mathbf{k}+\mathbf{q})]\cdot\mathbf{R}_i} \times (\mathbf{S}_i \cdot \boldsymbol{\sigma})_{\sigma''\sigma'}\hat{G}^{\sigma\sigma''}_{\mathbf{k},\mathbf{k}'}(E). \tag{25}$$

Now upon multiplying $\hat{G}^{(0)}_{\mathbf{k}}(E)$ from left to Eq. (24) we get

$$\hat{G}^{\sigma\sigma'}_{\mathbf{k},\mathbf{k}+\mathbf{q}}(E) = \delta_{\mathbf{k},\mathbf{k}+\mathbf{q}}\delta_{\sigma\sigma'}\hat{G}^{(0)}_{\mathbf{k}}(E) - \frac{J}{2N}\sum_{i\mathbf{k}'\sigma''} e^{-i(\mathbf{k}-\mathbf{k}')\cdot\mathbf{R}_i}(\mathbf{S}_i \cdot \boldsymbol{\sigma})_{\sigma\sigma''}\hat{G}^{(0)}_{\mathbf{k}}(E)\hat{G}^{\sigma''\sigma'}_{\mathbf{k}',\mathbf{k}+\mathbf{q}}(E) \tag{26}$$

and on multiplying $\hat{G}^{(0)}_{\mathbf{k}+\mathbf{q}}(E)$ from right to Eq. (25) we obtain

$$\hat{G}^{\sigma\sigma'}_{\mathbf{k},\mathbf{k}+\mathbf{q}}(E) = \delta_{\mathbf{k},\mathbf{k}+\mathbf{q}}\delta_{\sigma\sigma'}\hat{G}^{(0)}_{\mathbf{k}+\mathbf{q}}(E) - \frac{J}{2N}\sum_{i\mathbf{k}'\sigma''} e^{-i(\mathbf{k}'-(\mathbf{k}+\mathbf{q}))\cdot\mathbf{R}_i} \times (\mathbf{S}_i \cdot \boldsymbol{\sigma})_{\sigma''\sigma'}\hat{G}^{\sigma\sigma''}_{\mathbf{k},\mathbf{k}'}(E)\hat{G}^{(0)}_{\mathbf{k}+\mathbf{q}}(E). \tag{27}$$

Let us make the following crucial first-order approximations for the Green's functions:

$$\hat{G}^{\sigma\sigma''}_{\mathbf{k},\mathbf{k}'}(E) \approx \delta_{\sigma\sigma''}\delta_{\mathbf{k},\mathbf{k}'}\hat{G}_{\mathbf{k}\sigma}(E), \tag{28}$$

$$\hat{G}^{\sigma''\sigma'}_{\mathbf{k}',\mathbf{k}+\mathbf{q}}(E) \approx \delta_{\sigma''\sigma'}\delta_{\mathbf{k}',\mathbf{k}+\mathbf{q}}\hat{G}_{\mathbf{k}+\mathbf{q}\sigma'}(E), \tag{29}$$

where

$$\hat{G}_{\mathbf{k}\sigma}(E) = [E\hat{I} - \hat{\epsilon}(\mathbf{k}) - \hat{\Sigma}_{\sigma}(E)]^{-1}, \tag{30}$$

$$\hat{G}_{\mathbf{k}+\mathbf{q}\sigma'}(E) = [E\hat{I} - \hat{\epsilon}(\mathbf{k}+\mathbf{q}) - \hat{\Sigma}_{\sigma'}(E)]^{-1}. \tag{31}$$

The renormalization by the interacting Green's functions as performed in Eqs. (28) and (29) should be a sensible approximation since it is observed that if those interacting Green's functions are replaced by the free Green's functions Eqs. (22) and (23), respectively, then it leads to the correct low-J (i.e., RKKY) behavior. On substituting Eq. (29) in Eq. (26) we obtain

$$\hat{G}^{\sigma\sigma'}_{\mathbf{k},\mathbf{k}+\mathbf{q}}(E) = \delta_{\mathbf{q},0}\delta_{\sigma\sigma'}\hat{G}^{(0)}_{\mathbf{k}}(E) - \frac{J}{2N}\sum_{i} e^{i\mathbf{q}\cdot\mathbf{R}_i}(\mathbf{S}_i \cdot \boldsymbol{\sigma})_{\sigma\sigma'}\hat{G}^{(0)}_{\mathbf{k}} \times (E)\hat{G}_{\mathbf{k}+\mathbf{q}\sigma'}(E), \tag{32}$$

while substituting Eq. (28) in Eq. (27) gives

$$\hat{G}^{\sigma\sigma'}_{\mathbf{k},\mathbf{k}+\mathbf{q}}(E) = \delta_{\mathbf{q},0}\delta_{\sigma\sigma'}\hat{G}^{(0)}_{\mathbf{k}}(E) - \frac{J}{2N}\sum_{i} e^{i\mathbf{q}\cdot\mathbf{R}_i}(\mathbf{S}_i \cdot \boldsymbol{\sigma})_{\sigma\sigma'}\hat{G}_{\mathbf{k}\sigma}(E)\hat{G}^{(0)}_{\mathbf{k}+\mathbf{q}}(E). \tag{33}$$

On adding Eq. (32) and Eq. (33) we get

$$\hat{G}^{\sigma\sigma'}_{\mathbf{k},\mathbf{k}+\mathbf{q}}(E) = \delta_{\mathbf{q},0}\delta_{\sigma\sigma'}\hat{G}^{(0)}_{\mathbf{k}}(E) - \frac{J}{4N}\sum_i e^{i\mathbf{q}\cdot\mathbf{R}_i}(\mathbf{S}_i\cdot\boldsymbol{\sigma})_{\sigma\sigma'}\hat{A}^{\sigma\sigma'}_{\mathbf{k},\mathbf{k}+\mathbf{q}}(E), \quad (34)$$

where

$$\hat{A}^{\sigma\sigma'}_{\mathbf{k},\mathbf{k}+\mathbf{q}}(E) = [\hat{G}^{(0)}_{\mathbf{k}}(E)\hat{G}_{\mathbf{k}+\mathbf{q}\sigma'}(E) + \hat{G}_{\mathbf{k}\sigma}(E)\hat{G}^{(0)}_{\mathbf{k}+\mathbf{q}}(E)]. \quad (35)$$

For the effective spin Hamiltonian in Eq. (15), we need the expectation value $\langle c^{\dagger}_{\mathbf{k}+\mathbf{q}\alpha\sigma'}c_{\mathbf{k}\alpha\sigma}\rangle$, which we express in terms of the trace of imaginary part of the Green's function Eq. (34) by exploiting the spectral theorem[37]

$$\begin{aligned}\frac{1}{N}\sum_{\mathbf{k}}\langle c^{\dagger}_{\mathbf{k}+\mathbf{q}\alpha\sigma'}c_{\mathbf{k}\alpha\sigma}\rangle &= -\frac{1}{\pi N}\mathrm{Im\ Tr}\int_{-\infty}^{\infty}dEf_{-}(E)\sum_{\mathbf{k}}\hat{G}^{\sigma\sigma'}_{\mathbf{k},\mathbf{k}+\mathbf{q}}(E)\\ &= \delta_{\mathbf{q},0}\delta_{\sigma\sigma'}\left(\frac{-1}{\pi N}\right)\mathrm{Im\ Tr}\int_{-\infty}^{\infty}dEf_{-}(E)\sum_{\mathbf{k}}\hat{G}^{(0)}_{\mathbf{k}}(E)\\ &\quad + \frac{J}{4\pi N^2}\sum_i\left[e^{i\mathbf{q}\cdot\mathbf{R}_i}(\mathbf{S}_i\cdot\boldsymbol{\sigma})_{\sigma\sigma'}\mathrm{Im\ Tr}\right.\\ &\quad \left.\times\int_{-\infty}^{\infty}dEf_{-}(E)\sum_{\mathbf{k}}\hat{A}^{\sigma\sigma'}_{\mathbf{k},\mathbf{k}+\mathbf{q}}(E)\right]. \quad (36)\end{aligned}$$

On substituting Eq. (36) in Eq. (15) we get

$$\begin{aligned}H_f &= \frac{J}{2\pi N}\sum_{i\sigma\sigma'}\delta_{\sigma\sigma'}(\mathbf{S}_i\cdot\boldsymbol{\sigma})_{\sigma\sigma'}\ \mathrm{Im\ Tr}\int_{-\infty}^{\infty}dEf_{-}(E)\sum_{\mathbf{k}}\hat{G}^{(0)}_{\mathbf{k}}(E)\\ &\quad - \frac{J^2}{8\pi N^2}\sum_{ij\mathbf{q}\sigma\sigma'}\left[e^{-i\mathbf{q}\cdot(\mathbf{R}_i-\mathbf{R}_j)}(\mathbf{S}_i\cdot\boldsymbol{\sigma})_{\sigma'\sigma}(\mathbf{S}_j\cdot\boldsymbol{\sigma})_{\sigma\sigma'}\ \mathrm{Im\ Tr}\right.\\ &\quad \left.\times\int_{-\infty}^{\infty}dEf_{-}(E)\sum_{\mathbf{k}}\hat{A}^{\sigma\sigma'}_{\mathbf{k},\mathbf{k}+\mathbf{q}}(E)\right], \quad (37)\end{aligned}$$

i.e.,

$$H_f = -\frac{J}{2}\sum_{i\sigma}(\mathbf{S}_i\cdot\boldsymbol{\sigma})_{\sigma\sigma}\langle n^{(0)}_{\sigma}\rangle + \frac{J^2}{8N}\sum_{ij\mathbf{q}\sigma\sigma'}e^{-i\mathbf{q}\cdot(\mathbf{R}_i-\mathbf{R}_j)}\times(\mathbf{S}_i\cdot\boldsymbol{\sigma})_{\sigma'\sigma}(\mathbf{S}_j\cdot\boldsymbol{\sigma})_{\sigma\sigma'}D^{\sigma\sigma'}_{\mathbf{q}}, \quad (38)$$

where

$$\langle n^{(0)}_{\sigma}\rangle = -\frac{1}{\pi}\mathrm{Im\ Tr}\int_{-\infty}^{\infty}dEf_{-}(E)\frac{1}{N}\sum_{\mathbf{k}}\hat{G}^{(0)}_{\mathbf{k}}(E) \quad (39)$$

and

$$D^{\sigma\sigma'}_{\mathbf{q}} = -\frac{1}{\pi}\mathrm{Im\ Tr}\int_{-\infty}^{\infty}dEf_{-}(E)\frac{1}{N}\sum_{\mathbf{k}}\hat{A}^{\sigma\sigma'}_{\mathbf{k},\mathbf{k}+\mathbf{q}}(E). \quad (40)$$

If we perform spin summations on the right-hand side of Eq. (38) we obtain

$$H_f = -\frac{J}{2}\sum_i(\langle n^{(0)}_{\uparrow}\rangle - \langle n^{(0)}_{\downarrow}\rangle)S^z_i + \frac{J^2}{8N}\sum_{ij\mathbf{q}}e^{-i\mathbf{q}\cdot(\mathbf{R}_i-\mathbf{R}_j)}[D^{\downarrow\uparrow}_{\mathbf{q}}S^-_iS^+_j + D^{\downarrow\uparrow}_{\mathbf{q}}S^+_iS^-_j + (D^{\uparrow\uparrow}_{\mathbf{q}} + D^{\downarrow\downarrow}_{\mathbf{q}})S^z_iS^z_j], \quad (41)$$

where the spin operators S^{ζ}_i ($\zeta = +, -, z$) satisfy the usual commutation relations. The first term in the above equation is exactly zero since the free system is unpolarized. This finally yields an effective anisotropic Heisenberg-type spin Hamiltonian, which can be written as follows:

$$H_f = -\sum_{ij}[J^{(1)}_{ij}S^-_iS^+_j + J^{(2)}_{ij}S^+_iS^-_j + J^{(3)}_{ij}S^z_iS^z_j], \quad (42)$$

where

$$J^{(n)}_{ij} = \frac{1}{N}\sum_{\mathbf{q}}J^{(n)}(\mathbf{q})e^{-i\mathbf{q}\cdot(\mathbf{R}_i-\mathbf{R}_j)} \quad (n=1,2,3) \quad (43)$$

with

$$J^{(1)}(\mathbf{q}) = -\frac{J^2}{8}D^{\uparrow\downarrow}_{\mathbf{q}}, \quad (44)$$

$$J^{(2)}(\mathbf{q}) = -\frac{J^2}{8}D^{\downarrow\uparrow}_{\mathbf{q}}, \quad (45)$$

$$J^{(3)}(\mathbf{q}) = -\frac{J^2}{8}(D^{\uparrow\uparrow}_{\mathbf{q}} + D^{\downarrow\downarrow}_{\mathbf{q}}), \quad (46)$$

are the effective exchange integrals, which, via $G_{\mathbf{k}\sigma}$, are functionals of the conduction-electron self-energy thereby getting a temperature and carrier-concentration dependence. In order to obtain effective isotropic Heisenberg-type spin Hamiltonian, one can prove[39] that $D^{\uparrow\downarrow}_{\mathbf{q}} = D^{\downarrow\uparrow}_{\mathbf{q}}$ and $D^{\uparrow\uparrow}_{\mathbf{q}} + D^{\downarrow\downarrow}_{\mathbf{q}} = 2D^{\downarrow\uparrow}_{\mathbf{q}}$, which will result in $J^{(1)}(\mathbf{q}) = J^{(2)}(\mathbf{q}) = J^{(3)}(\mathbf{q})/2 = J^{\mathrm{eff}}(\mathbf{q})$. We finally get

$$H_f = -\sum_{ij}^{n.n}J^{\mathrm{eff}}_{ij}\left[\frac{1}{2}(S^-_iS^+_j + S^+_iS^-_j) + S^z_iS^z_j\right]. \quad (47)$$

Now so as to determine the f spin magnetization, we follow along the lines of Callen[40] that results in

$$\langle S^z\rangle = \frac{(S-\varphi)(1+\varphi)^{2S+1} + (S+1+\varphi)\varphi^{2S+1}}{(1+\varphi)^{2S+1} - \varphi^{2S+1}}, \quad (48)$$

where $\varphi(S)$ can be interpreted as average magnon number

$$\varphi(S) = \frac{1}{N}\sum_{\mathbf{q}}\frac{1}{e^{E(\mathbf{q})/k_BT} - 1} \quad (49)$$

depending on S via magnon energies $E(\mathbf{q})$, which can be obtained using the spin Green's function[40] and is given by

$$E(\mathbf{q}) = 2\langle S^z\rangle[J^{\mathrm{eff}}(0) - J^{\mathrm{eff}}(\mathbf{q})], \quad (50)$$

with $J^{\mathrm{eff}}(0) = J^{\mathrm{eff}}(\mathbf{q}=0)$. In Sec. II A, we observed that the magnetization ($\langle S^z\rangle$) appears in electronic self-energy and this self-energy is used to calculate the exchange integrals, which along with $\langle S^z\rangle$ enter the magnon energies. These magnon energies in turn also appear in $\langle S^z\rangle$. Thus, we have

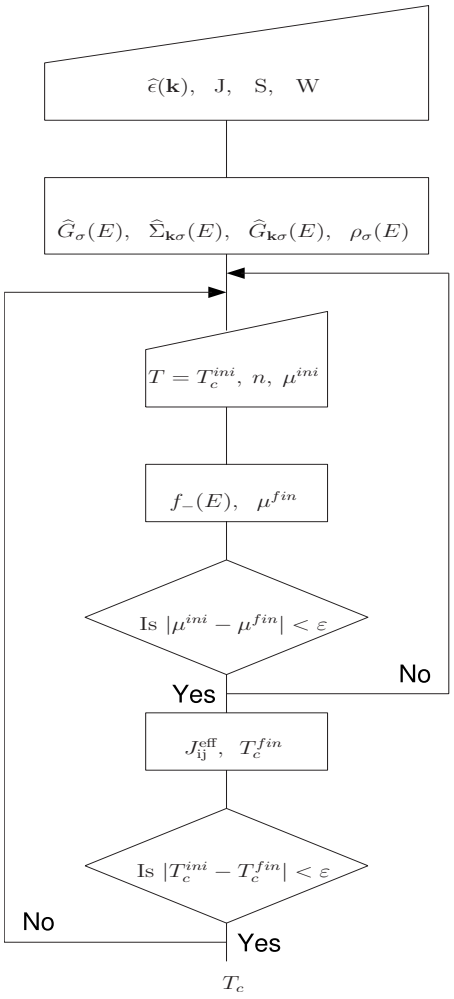

FIG. 2. Flowchart exhibiting the self-consistent determination of Curie temperature T_c. The terminologies are as explained in the text.

found a closed system of equations that can be solved self-consistently for all quantities of interest, in particular those which tell us about the mutual influence of electronic and magnetic properties of the exchange-coupled system of itinerant electrons and localized f spins.

One of the central quantities in magnetic system is the Curie temperature T_c, which can be ascribed to the temperature for which $\langle S^z \rangle \to 0$. On expanding Eq. (48) in $\frac{1}{\varphi(S)}$ we get

$$\langle S^z \rangle = \frac{S(S+1)}{3\varphi(S)} + O\left(\frac{1}{[\varphi(S)]^2}\right). \tag{51}$$

For $\langle S^z \rangle \to 0$ we have

$$e^{E(\mathbf{q})/k_B T} \simeq 1 + \frac{E(\mathbf{q})}{k_B T}. \tag{52}$$

Using Eqs. (49)–(52) we obtain

$$T_c = \frac{2S(S+1)}{3k_B}\left\{\frac{1}{N}\sum_{\mathbf{q}}\left[\frac{1}{[J^{\text{eff}}(0) - J^{\text{eff}}(\mathbf{q})]}\right]_{T_c}\right\}^{-1}. \tag{53}$$

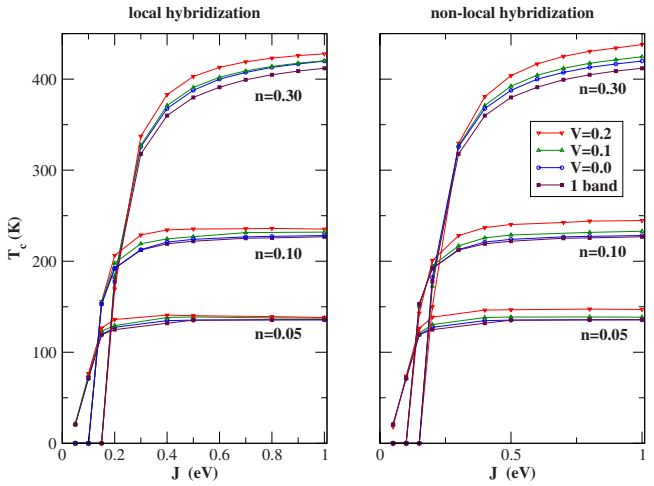

FIG. 3. (Color online) The dependence of Curie temperature (T_c) on intra-atomic exchange (J) for different values of band occupation. The exhibited results are for single- and two-band KLMs with local (left panel) and nonlocal hybridization (right panel) on a sc lattice.

We can evaluate Eq. (53) within a self-consistent cycle as shown in Fig. 2, which can be understood as follows. In our analysis we consider a two-band model (α and $\nu = 1,2$), which can be generalized to a n-band model. The single-particle energies $\hat{\epsilon}(\mathbf{k})$ are then represented in a 2×2 matrix where the diagonal and nondiagonal terms are considered to have the following form: $\epsilon^{11}(\mathbf{k}) = -\frac{W}{6}[\cos(k_x a) + \cos(k_y a) + \cos(k_z a)]$, $\epsilon^{12}(\mathbf{k}) = \epsilon^{21}(\mathbf{k}) = V$ (local hybridization, LH) or $\epsilon^{12}(\mathbf{k}) = \epsilon^{21}(\mathbf{k}) = V\epsilon^{11}(\mathbf{k})$ (nonlocal hybridization, NLH), and $\epsilon^{22}(\mathbf{k}) = E_0 + \epsilon^{11}(\mathbf{k})$. Along with the single-particle energies, the intra-atomic exchange J, quantum spin number S, and bandwidth W act as input parameters in order to evaluate the free propagator, self-energy, and full propagator. Then for a particular band occupation n and an initial temperature T_c^{ini}, the Fermi edge μ, which yields the correct value of n, is determined self-consistently. Thus, fixing upon the Fermi edge one evaluates the temperature-dependent exchange integrals, which gives the T_c through Eq. (53). If the obtained temperature is within convergence limit ε, then it is the resulting T_c for particular J and n.

III. RESULTS & DISCUSSION

On optimizing the numerical factor,[41] we evaluate the Curie temperature, i.e., Eq. (53) for various configurations of model parameters (J, n, and V). We consider the spin quantum number $S = \frac{7}{2}$ (localized moment of Eu^{2+} and Gd^{3+}) and the center of gravity of the second band shifted by an amount $E_0 = 0.25$ eV. First we try to reproduce the single-band result for different values of band occupation (as was previously obtained) but using another electronic self-energy.[42] This will give us some confidence on the working of the algorithm.

Figure 3 shows the dependence of T_c on the strength of intra-atomic exchange J for single- and two-band KLM. The left panel describes the results for LH while the right panel for NLH on a simple-cubic (sc) lattice. The bandwidth of both the bands W is taken to be 1.0 eV. The calculations are

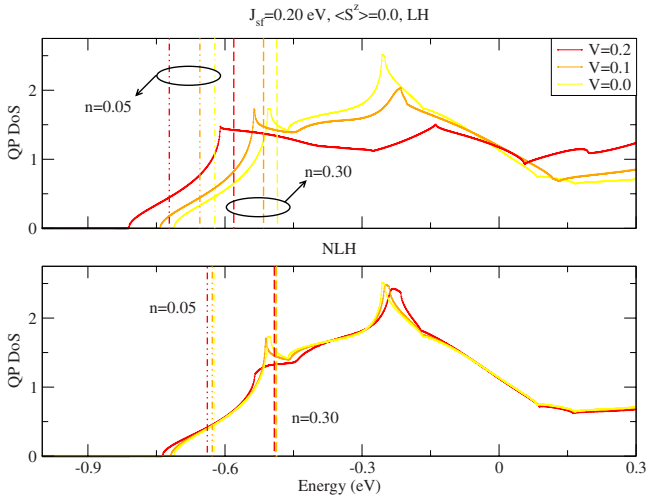

FIG. 4. (Color online) Lower edge of paramagnetic density of states of two-band KLM with LH (upper panel) and NLH (lower panel) on a sc lattice for $J=0.20$ eV. The curves and vertical lines in yellow, orange, and red are for $V=0.0$, 0.1, and 0.2, respectively. The vertical lines denote the Fermi edge with dashed-dotted and dashed lines for band occupations n of 0.05 and 0.30, respectively.

carried out for different values of band occupation n and hybridization V.

Although both the graphs look quite similar, there are marked differences especially in the limit of strong coupling and low-band occupation. We first discuss the general behavior. It is observed that initially the T_c rises sharply with increasing J. For weak coupling and small-band occupation ($n=0.05$), the usual RKKY mechanism is observed. However for higher-band occupation, J is observed to exceed a critical value in order to allow ferromagnetism. Furthermore, with increasing J the critical temperature is observed to be deviating more and more from the RKKY behavior (i.e., long-range order) and finally reaches a saturation. The calculations done within single-band model are comparable with previous calculations[42] obtained using a different self-energy.

As shown in Fig. 3, the results for T_c in case of two unhybridized bands ($V=0.0$) are in comparison with that of the one-band situation for low-band occupation due to similar low-energy paramagnetic density of states at the Fermi edge and with increasing band occupation, the results in both the situation (local and nonlocal hybridization) differ drastically. The values of Curie temperatures are found to be higher and increasing with increasing hybridization strength and band occupation for two hybridized bands as compared to the unhybridized or one-band model. It can be understood as follows.

Figure 4 shows the low-energy window of the paramagnetic density of states of two-band KLM with local and nonlocal hybridization shown in upper and lower panels, respectively. The calculations are performed for $J=0.20$ eV. The curves and vertical lines in yellow, orange, and red are for $V=0.0$, 0.1, and 0.2, respectively. The vertical lines signify the Fermi edge with dashed-dotted and dashed lines for band occupations of 0.05 and 0.30, respectively. The lines within the circle represent the Fermi edge for different values of hybridization but for the same value of band occupation.

It is to be noted that in general the shape of the density of states is dependent on the band occupation, which is a consequence of electronic correlation effects. But the self-energy, which we consider in our calculations, is independent of band occupation or rather well defined only in the limit of low-band occupation. Since we restrict ourselves to this limit, thus, we have density of states dependent only on the strength of hybridization. The band filling is determined by the placement of Fermi edge, which is obtained self-consistently in our calculations. In order to improve over the restricted limit, we can consider the band-occupation-dependent self-energy as given in Ref. 43 but this is not the aim of the present paper.

We observe that for low-band occupation, the density of states at the Fermi edge is slightly different for different values of hybridization. But with increasing band occupation, the density of states at the Fermi edge changes abruptly for local as well as for nonlocal hybridization.

Although for high-band occupation the values of T_c in case of two hybridized bands are higher as compared to unhybridized or one-band situation, but for low-band occupation and strong-coupling limit, an interesting feature is observed as shown (encircled) in Fig. 5. Since it is only observed in case of two locally hybridized bands, we do not consider the case of nonlocal hybridization. It is noted that in the limit of strong coupling, the T_c starts decreasing for two hybridized band system as compared to two unhybridized band model. Even though increasing hybridization increases the bandwidth and therefore the kinetic energy of the itinerant electrons, it is only effective for higher-band occupation. In the regime of low-band occupation and strong coupling, the short-range order due to strong intra-atomic exchange and local hybridization decreases the kinetic energy leading to localization of the carrier. This results in decrease in the paramagnetic density of states at the Fermi edge, thereby reducing the T_c to the value of the one-band case, which is encircled in the left-most panel in Fig. 5. But as mentioned earlier, upon increasing the band occupation (moving to the right panels) we observe that the T_c increases with increase in hybridization (bandwidth)[42] and also in the limit of strong coupling due to the presence of more delocalized electrons. It can be again understood within the picture of the density of states.

Figure 6 shows the low-energy spectrum of paramagnetic density of states for two locally hybridized band KLM on a sc lattice for $J=0.80$ eV. The curves and vertical lines in yellow, orange, and red are for $V=0.0$, 0.1, and 0.2, respectively. The vertical lines denote the Fermi edge with dashed-dotted and dashed lines for band occupations of 0.10 and 0.50, respectively. As observed for $n=0.10$ the density of states at the Fermi edge is slightly different giving rise to marginal difference in T_c with increase in hybridization. But with increasing band occupation ($n=0.50$), the density of states at the Fermi edge differs drastically giving rise to quite different Curie temperatures.

Another feature, which we observe in the strong-coupling limit, is that the density of states tends to separate out with increasing value of hybridization as shown in Fig. 6 but the change from $V=0.1$ to $V=0.2$ is quite sudden. In order to have a close look at it, we plot the paramagnetic density of

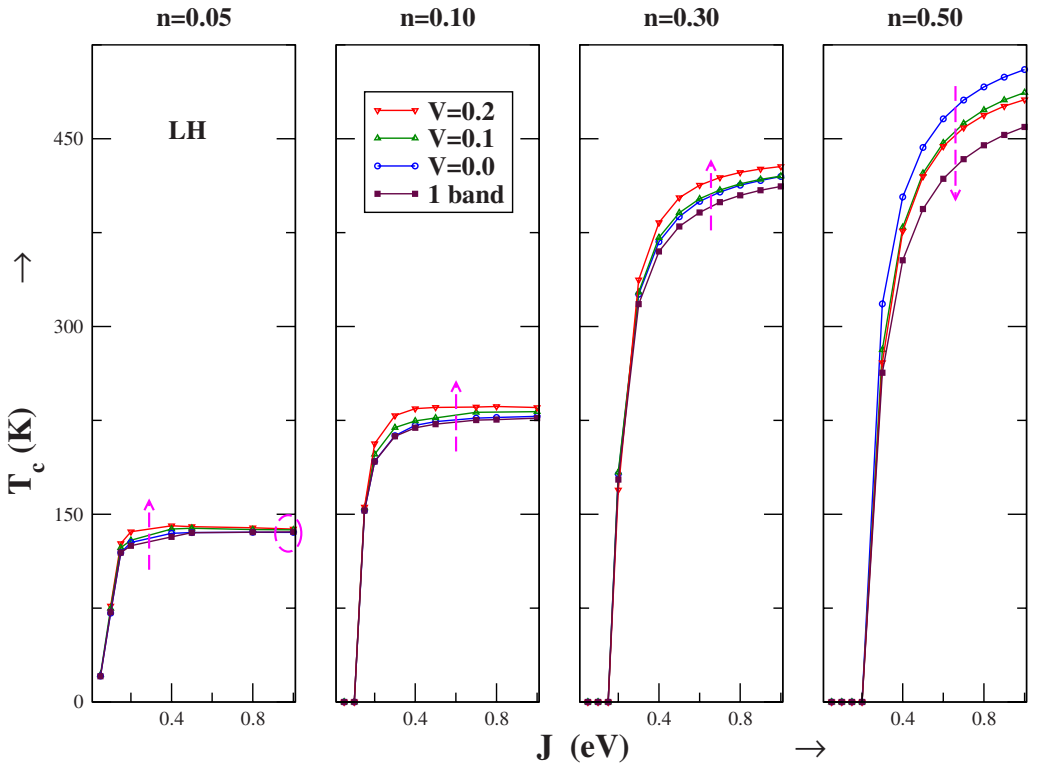

FIG. 5. (Color online) The same as in Fig. 3 but only for LH and an additional result for band occupation of $n=0.50$.

states for $J=0.80$ eV and intermediate values of hybridization from $V=0.1$ to $V=0.2$ as shown in Fig. 7. It is noted that there is an increase in bandwidth with increasing hybridization.

Further interesting characteristic is observed for band occupation of $n=0.50$. It is seen that the trend of higher and increasing value of T_c for two locally hybridized band model is reversed as shown in the right-most panel of Fig. 5. As the Fermi edge keeps on moving to higher energies with an increase in band occupation, the paramagnetic density of states at the Fermi edge keeps on changing. This results in an observed change in the T_c. A similar pattern of decrease in the value of Curie temperature with increase in band occupation and strength of hybridization is also observed in case of nonlocal hybridization. The explanation lies similar to what we have explained earlier in case of local hybridization.

On the other hand since T_c is directly related to effective exchange integrals J_{ij}^{eff}, it is also interesting to notice the behavior of these exchange integrals for different values of

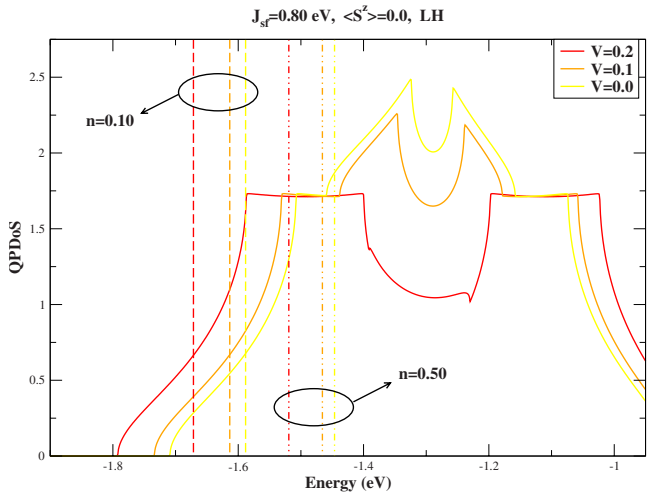

FIG. 6. (Color online) Lower edge of paramagnetic density of states for two locally hybridized band KLM on a sc lattice for $J=0.80$ eV. The curves and vertical lines in yellow, orange, and red are for $V=0.0$, 0.1, and 0.2, respectively. The vertical lines denote the Fermi edge with dashed-dotted and dashed lines for band occupations n of 0.10 and 0.50, respectively.

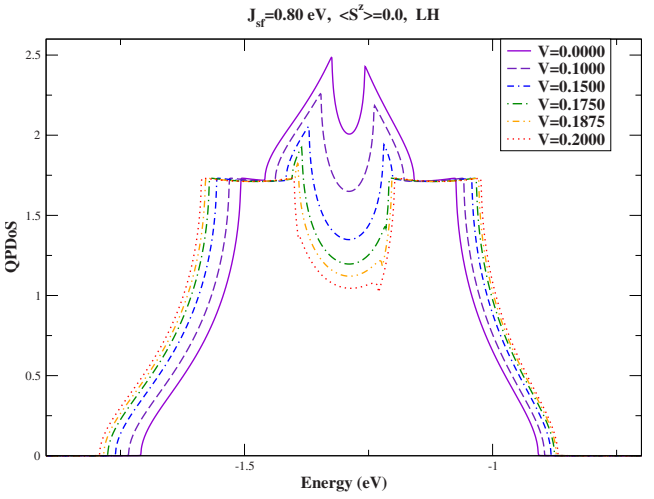

FIG. 7. (Color online) Lower edge of paramagnetic density of states for two locally hybridized band KLM on a sc lattice for $J=0.80$ eV and for different values of hybridization.

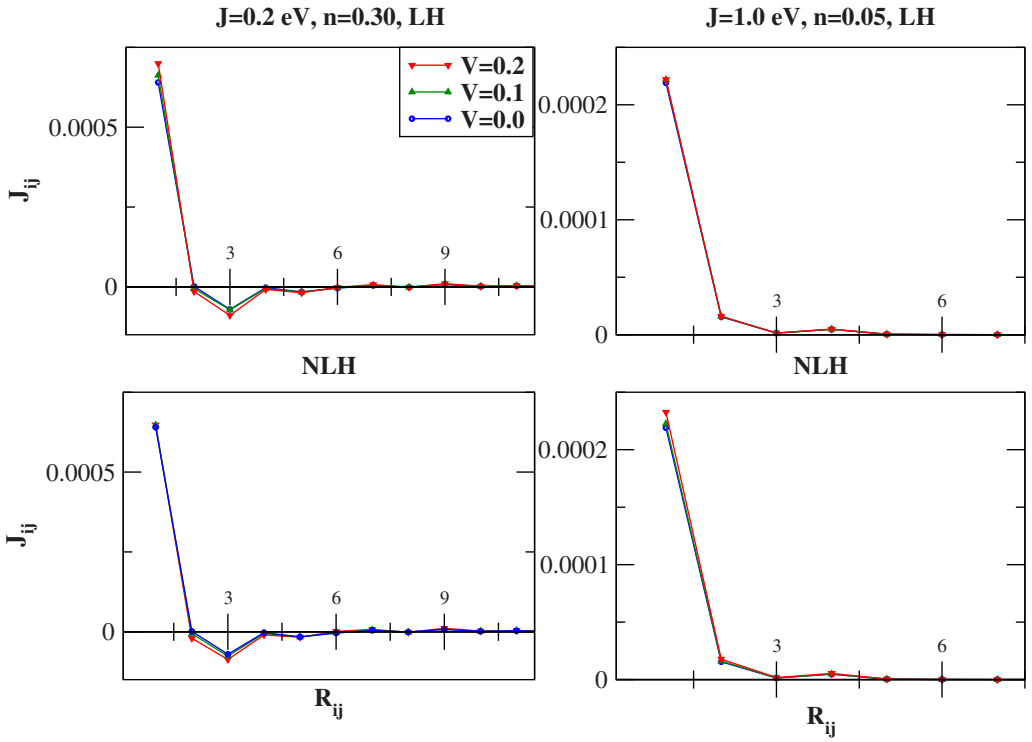

FIG. 8. (Color online) The indirect exchange integrals shown as a function of distance for local (upper panel) and nonlocal hybridization (lower panel). The shown results are for two different values of intra-atomic exchange and band occupation but for three different values of hybridization.

n, J, and V and for local as well as nonlocal hybridization. Figure 8 shows the dependence of indirect effective exchange integrals on two different parameter configuration of J and n and for three different values of hybridization. We observe the long-range RKKY kind of oscillations[33] for weak coupling in case of local and nonlocal hybridization. In case of strong coupling, the local short-range order is stronger. In that case, the exchange integrals get converged very quickly within a short distance.

IV. SUMMARY & CONCLUSION

In this paper, we studied the magnetic properties of the multiband Kondo lattice model Hamiltonian, which describes the intra-atomic exchange interaction between itinerant electrons and localized spins on a periodic lattice. In Sec. II A, we considered only the electronic part of the system. Using an earlier proposed ansatz for multiband self-energy,[35] we evaluated the electronic properties of interest such as the density of states and band occupation number. In Sec. II B, we developed the modified RKKY theory[36] wherein we integrated out the charge degrees of freedom of the itinerant electrons thereby mapping the multiband Kondo lattice model Hamiltonian onto an effective Heisenberg-type spin Hamiltonian. In Sec. III, using this procedure we determined the magnetic properties of the system such as Curie temperature (within random phase approximation) for various values of system parameters while calculating the chemical potential and magnetization within a self-consistent scheme.

We found that the T_c as a function of intra-atomic exchange J for a two-band KLM remains qualitatively the same for local as well as nonlocal hybridization between both the bands, except for the limit of low-band occupation and strong coupling. For higher-band occupation and increase in strength of coupling as well as hybridization, we find that T_c increases until the band occupation of $n=0.5$ from where the trend is reversed. All these can be explained using the paramagnetic density of states and its behavior at the Fermi edge. It is mainly due to the interplay between kinetic and potential energy. In case of strong coupling, the T_c is oscillating in its dependence on the band occupation.

Such an analysis can be very useful in order to understand the physical properties of real materials described within the multiband models such as the manganites (these materials are known to have a strong intra-atomic exchange coupling behavior) or the analysis can be equally handful for the rare-earth metals, which are known to be described within the weak or intermediate intra-atomic coupling regime. It would be equally encouraging to carry out the similar investigation for two different bandwidths of both the bands since the correlation effects scale as $\frac{J}{W}$, where W being the bandwidth.

We would also like to apply[44] the multiband modified RKKY theory in order to understand the basic mechanism behind the observed ferromagnetism in GdN.[45,46]

ACKNOWLEDGMENTS

One of the authors (A.S.) benefited from valuable discussions on the numerical calculations with Sören Henning and Jochen Kienert.

*anand@physik.hu-berlin.de

[1] J. Kondo, Prog. Theor. Phys. **32**, 37 (1964).
[2] N. Furukawa, J. Phys. Soc. Jpn. **63**, 3214 (1994).
[3] E. Dagotto, S. Yunoki, A. L. Malvezzi, A. Moreo, J. Hu, S. Capponi, D. Poilblanc, and N. Furukawa, Phys. Rev. B **58**, 6414 (1998).
[4] T. Kasuya, Prog. Theor. Phys. **16**, 45 (1956).
[5] K. Yosida, Phys. Rev. **106**, 893 (1957).
[6] W. Nolting, Phys. Status Solidi B **96**, 11 (1979).
[7] E. L. Nagaev, *Physics of Magnetic Semiconductors* (Mir, Moscow, 1983).
[8] P. Wachter, *Handbook on the Physics and Chemistry of Rare Earth* (North-Holland, Amsterdam, 1979), Chap. 19.
[9] A. Mauger and C. Godart, *Physics Reports (Review Section of Physics Letters)* (North-Holland, Amsterdam, 1986), Vol. 141, pp. 51–176.
[10] W. Müller and W. Nolting, Phys. Rev. B **69**, 155425 (2004).
[11] T. Dietl and H. Ohno, MRS Bull. **28**, 714 (2003).
[12] G. Tang and W. Nolting, Phys. Rev. B **75**, 024426 (2007).
[13] A. Singh, S. K. Das, A. Sharma, and W. Nolting, J. Phys.: Condens. Matter **19**, 236213 (2007).
[14] S. A. Wolf, D. D. Awschalom, R. A. Buhrman, J. M. Daughton, S. von Molnàr, M. L. Roukes, A. Y. Chtchelkanova, and D. M. Treger, Science **294**, 1488 (2001).
[15] I. Žutic, J. Fabian, and S. Das Sarma, Rev. Mod. Phys. **76**, 323 (2004).
[16] S. Rex, V. Eyert, and W. Nolting, J. Magn. Magn. Mater. **192**, 529 (1999).
[17] C. Santos, W. Nolting, and V. Eyert, Phys. Rev. B **69**, 214412 (2004).
[18] D. Li, J. Zhang, P. A. Dowben, and M. Onellion, Phys. Rev. B **45**, 7272 (1992).
[19] *Magnetism and Electronic Correlations in Local Moment Systems: Rare Earth Elements and Compounds*, edited by M. Donath, P. Dowben, and W. Nolting (World Scientific, Singapore, 1998).
[20] S. Jin, T. H. Tiefel, M. McCormack, R. A. Fastnacht, R. Ramesh, and L. H. Chen, Science **264**, 413 (1994).
[21] A. P. Ramirez, J. Phys.: Condens. Matter **9**, 8171 (1997).
[22] C. Zener, Phys. Rev. **81**, 440 (1951); P. W. Anderson and H. Hasegawa, *ibid.* **100**, 675 (1955); P. G. de Gennes, *ibid.* **118**, 141 (1960); K. Kubo and N. Ohata, J. Phys. Soc. Jpn. **33**, 21 (1972); N. Ohata, *ibid.* **34**, 343 (1973).
[23] M. Stier and W. Nolting, Phys. Rev. B **75**, 144409 (2007).
[24] H. von Löhneysen in Ref. 19.
[25] S. Doniach, Physica B & C **91**, 231 (1977).
[26] F. Popescu, Ph.D. thesis, Florida State University, 2007.
[27] H. Nagao, Int. J. Quantum Chem. **100**, 867 (2004).
[28] J. Hubbard, Proc. R. Soc. London, Ser. A **276**, 238 (1963).
[29] K. Penc, H. Shiba, F. Mila, and T. Tsukagoshi, Phys. Rev. B **54**, 4056 (1996).
[30] W. Nolting and W. Borgiel, Phys. Rev. B **39**, 6962 (1989).
[31] Y.-Q. Wang, H. Q. Lin, and J. E. Gubernatis, Comput. Phys. Commun. **1**, 575 (2006).
[32] P. W. Anderson, Phys. Rev. **124**, 41 (1961).
[33] M. A. Ruderman and C. Kittel, Phys. Rev. **96**, 99 (1954); T. Kasuya, Prog. Theor. Phys. **16**, 45 (1956).
[34] D. Meyer, W. Nolting, G. G. Reddy, and A. Ramakanth, Phys. Status Solidi B **208**, 473 (1998).
[35] A. Sharma and W. Nolting, J. Phys.: Condens. Matter **18**, 7337 (2006).
[36] W. Nolting, S. Rex, and S. Mathi Jaya, J. Phys.: Condens. Matter **9**, 1301 (1997).
[37] D. N. Zubarev, Usp. Fiziol. Nauk **71**, 71 (1960) [Sov. Phys. Usp. **3**, 320 (1960)].
[38] A. Sharma and W. Nolting, Phys. Status Solidi B **243**, 641 (2006). In this paper, the case of carriers in completely filled bands was considered. But it can be proved that the case of carriers in completely empty bands, as considered in present manuscript, is identical to that of the fully occupied bands.
[39] A. Sharma, Ph.D. thesis, Humboldt-Universität zu Berlin, 2007.
[40] H. B. Callen, Phys. Rev. **130**, 890 (1963).
[41] The small imaginary part has to be numerically optimized for low-band occupation and coupling strength.
[42] C. Santos and W. Nolting, Phys. Rev. B **65**, 144419 (2002).
[43] W. Nolting, G. G. Reddy, A. Ramakanth, D. Meyer, and J. Kienert, Phys. Rev. B **67**, 024426 (2003).
[44] A. Sharma and W. Nolting (unpublished).
[45] D. X. Li, Y. Haga, H. Shida, T. Suzuki, Y. S. Kwon, and G. Kido, J. Phys.: Condens. Matter **9**, 10777 (1997).
[46] S. Granville, B. J. Ruck, F. Budde, A. Koo, D. J. Pringle, F. Kuchler, A. R. H. Preston, D. H. Housden, N. Lund, A. Bittar, G. V. M. Williams, and H. J. Trodahl, Phys. Rev. B **73**, 235335 (2006).